Hindawi
Geofluids
Volume 2023, Article ID 4123836, 18 pages
https://doi.org/10.1155/2023/4123836

Research Article

Experimental Study of Complex Resistivity Characteristics of a Sandstone Reservoir under Different Measurement Conditions

Xinghao Wang, Kui Xiang, Yuanyuan Luo, Gongxian Tan, and Jiaju Ruan

Key Laboratory of Exploration Technologies for Oil and Gas Resources, Yangtze University, Wuhan 430100, China

Correspondence should be addressed to Kui Xiang; xiangkui@yangtzeu.edu.cn

Received 10 October 2022; Revised 1 November 2022; Accepted 24 November 2022; Published 4 February 2023

Academic Editor: Jianchao Cai

Copyright © 2023 Xinghao Wang et al. This is an open access article distributed under the Creative Commons Attribution License, which permits unrestricted use, distribution, and reproduction in any medium, provided the original work is properly cited.

Due to the variability of fluid properties and saturation of reservoirs, large differences in formation temperature and pressure, and the diversity of rock and mineral compositions, the petrophysical response of reservoirs is often complex. This study explored a new method of reservoir fluid identification and evaluation based on the complex resistivity response characteristics of sandstone reservoirs under different measurement conditions. The complex resistivity of the five sandstone samples was measured under normal temperature and pressure and variable pressure, temperature, and formation conditions and under different oil saturations. Furthermore, the reservoir was comprehensively analyzed and evaluated based on the mineral composition, porosity, and permeability parameters. The results show that the resistivity of the sandstone increases logarithmically with pressure and oil saturation but decreases logarithmically with temperature and depth. The polarizability decreases slightly with increasing pressure and increases slightly with increasing temperature. With increasing depth, the polarizability decreases obviously, and with increasing oil saturation, the polarizability decreases moderately. Under different measurement conditions, the complex resistivity data for the sandstone reservoir and the IP parameters extracted through inversion are regular. The results of this study provide a new method for the identification and evaluation of complex reservoir fluids and have important reference value.

1. Introduction

Since the frequency dispersion of the complex resistivity of rocks was discovered in the laboratory in the first half of the last century [1], the complex resistivity of rocks has become more and more widely used in various deep structures, resource exploration, and engineering geophysical prospecting [2, 3]. Scholars in China and abroad have also conducted extensive and in-depth research on the dispersion characteristics of complex resistivity [4–7]. Many factors affect the complex resistivity of rocks [8]. In recent decades, Chinese scholars have made many achievements in the study of the complex resistivity of rocks under simulated stratum conditions [9]. Revil et al. [10, 11] used a new model to study the influence of oil saturation of formation water on the complex resistivity of oil-bearing sandstone and found that the resistivity and the amplitude of the phase increase with increasing oil saturation, while the imaginary component of the complex resistivity decreases. Burtman and Zhdanov [12] found that oil-bearing sandstone and carbonate rocks have significant induced polarization response characteristics through experiments and verified the early geophysical application of the IP method in oil-bearing reservoir exploration. By measuring the complex resistivity of artificial sandstone with different physical properties under different water saturation conditions and by fitting the data using the Cole–Cole model, Jiang et al. [13] found that the frequency index in the model initially decreased and then increased with decreasing water saturation, so they pointed out that it is expected that this index is expected to be applied in the study of oil-water distribution in reservoirs. Brace and Orange [14] analyzed the influence of pressure as high as 10 kb on the resistivity of 30 kinds of crystalline rocks with great differences. It is found that porosity is the only property that determines the high-pressure resistivity of water-saturated rocks composed of nonconductive minerals. Liu et al. [15] systematically summarized and analyzed the influence of pressure and temperature on the conductivity

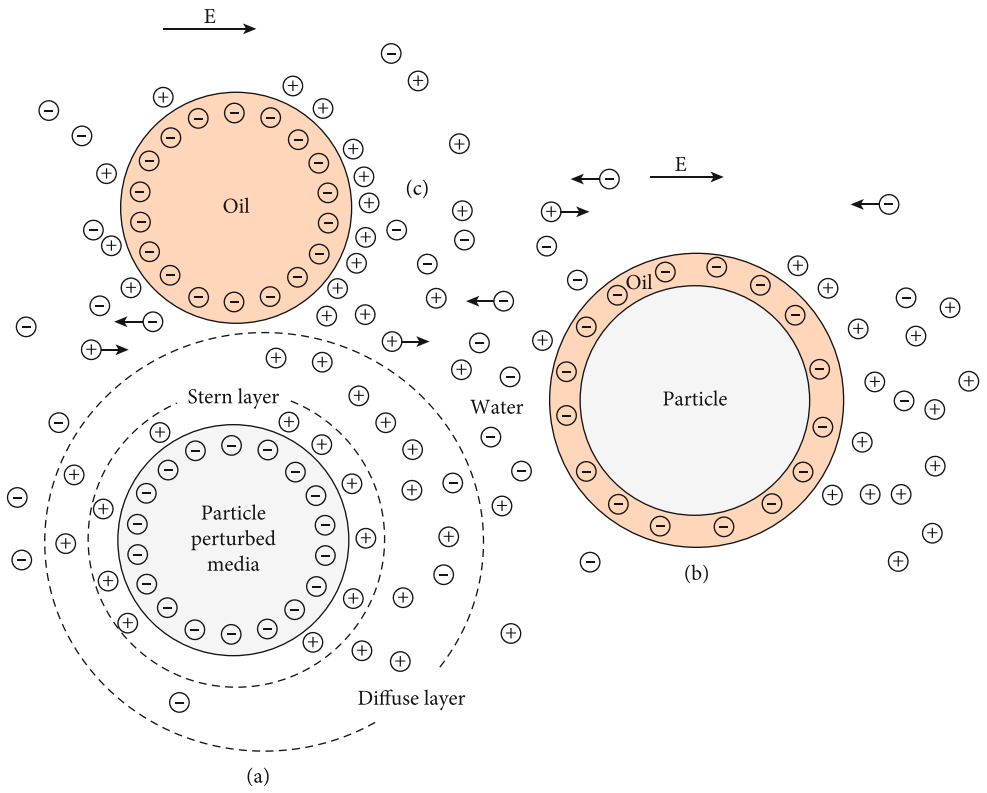

Figure 1: Diagram showing the distribution of the electric double layer under different wettability conditions: (a) the electric double layer distribution under hydrophilic conditions, (b) the electric double layer distribution under lipophilic conditions, and (c) the electric double layer at the oil-water interface [22].

and wave velocity of basalt. Li et al. [16] by measuring the anisotropic conductivity of artificial porous sandstone samples under pressure difference, the change of fracture parameters caused by the differential pressure and their influence on the anisotropic electrical conductivity of the rocks were further analyzed theoretically. The complex resistivity of argillaceous sandstone was tested and analyzed by Sun et al. [17] under high-temperature and high-pressure conditions, and the influences of the salinity and depth of the rock reservoir on the complex resistivity were obtained. Cheng et al. [18] studied the electrical characteristics of black shale in eastern Guizhou and identified the anisotropy of complex resistivity of the shale and its relationship with the shale's physical parameters. Wang et al. [19] measured the electrical properties of rocks under simulated high-temperature and high-pressure formation conditions and compared them with normal temperature and normal pressure conditions. They found that the electrical property indices measured under formation conditions were smaller than those measured under normal temperature and normal pressure conditions. The research objects of most previous studies were sandstone reservoirs [20], and some scholars have predicted the properties of clastic reservoirs using establishing models [21]. In terms of the electrochemical properties of rocks, it has been found that the wettability of the rock surface can affect the electric double layer between two-phase media, thus affecting the induced polarization (Figure 1) [22]. However, the subjects of the above research were relatively singular, and they failed to comprehensively discuss the complex resistivity response characteristics of rock samples from multiple angles. There are limitations in the research conducted on some unconventional reservoirs [23]. Therefore, by measuring and analyzing the complex resistivity response and polarizability of five sandstone samples under multiple measurement conditions, this study provides a more valuable reference for fluid identification and the evaluation of complex reservoirs.

Table 1: Basic information about rock samples.

Serial number	Core number	Lithology	Porosity	Permeability (mD)
1	Sample 01	Sandstone	12.90%	2.8550
2	Sample 02	Sandstone	13.38%	3.8997
3	Sample 03	Sandstone	10.14%	0.8549
4	Sample 04	Sandstone	8.60%	1.3839
5	Sample 05	Sandstone	9.16%	0.8186

2. Rock Samples and Experimental Methods

2.1. Experimental Rock Samples. Five sandstone reservoir samples from the Huabei Oilfield were used as the experimental basis in this study. The basic information about these samples is presented in Table 1.

The rock samples were numbered sample 01, sample 02, sample 03, sample 04, and sample 05 (Figure 2). From the

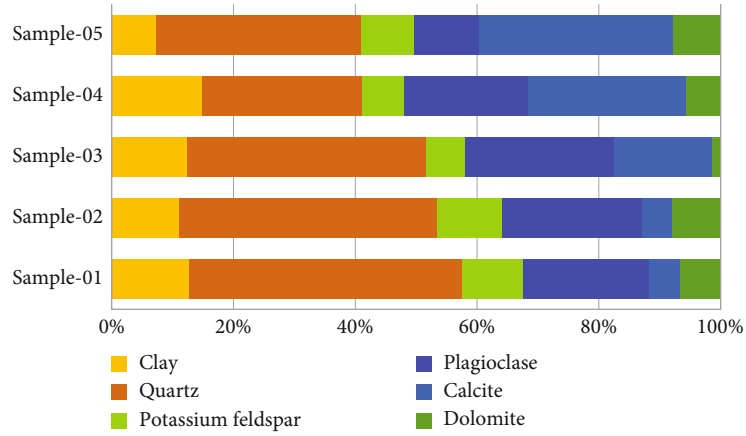

Figure 2: Mineral compositions of rock samples.

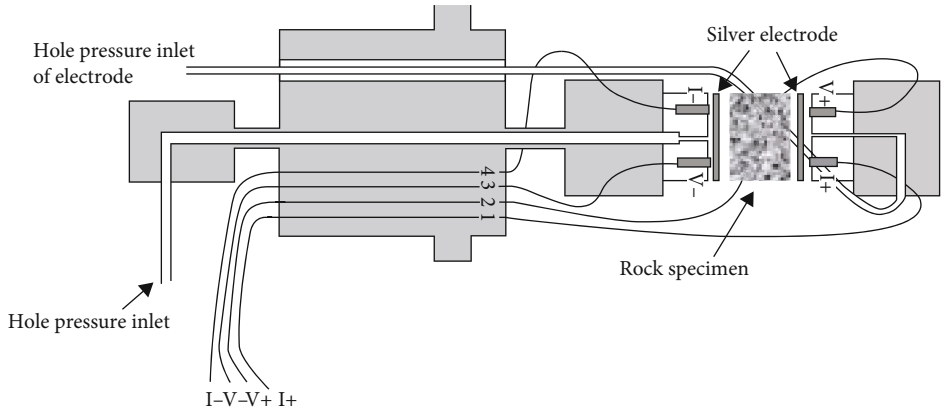

Figure 3: Schematic diagram showing the principle of the complex resistivity measurements.

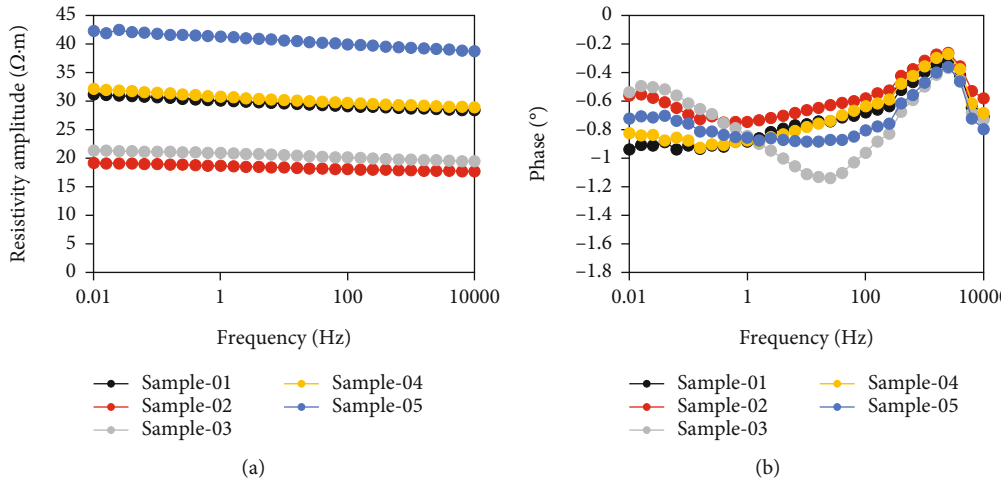

Figure 4: Amplitude and phase of complex resistivity of sandstone samples under normal temperature and pressure conditions: (a) complex resistivity amplitude curve and (b) complex resistivity phase curve.

basic porosity and permeability information for the rock samples and the distribution of their mineral compositions, it can be seen that the porosity and permeability of the experimental rock samples vary slightly. In terms of their mineral compositions, the proportion of quartz is relatively large, and the contents of plagioclase, calcite, dolomite, and potassium feldspar are different. The clay contents of the five rock samples are similar.

2.2. Complex Resistivity Measurement System. An Autolab 1000 and a 1260A impedance analyzer were used to measure the complex resistivity of the rocks. The equipment can

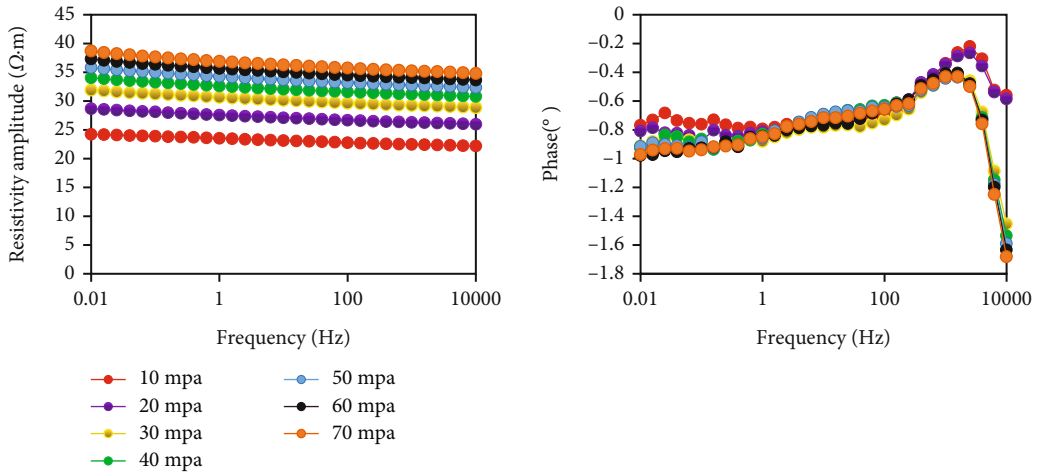

(a)

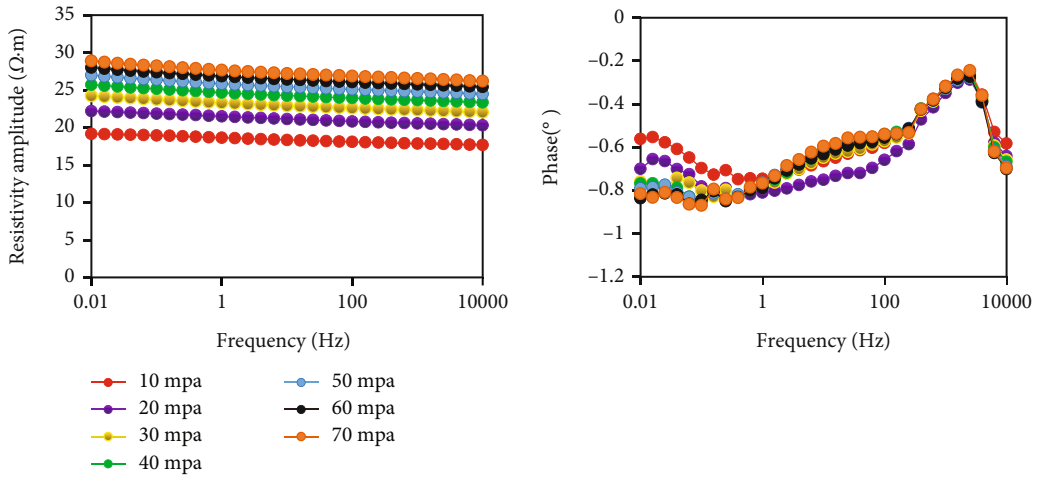

(b)

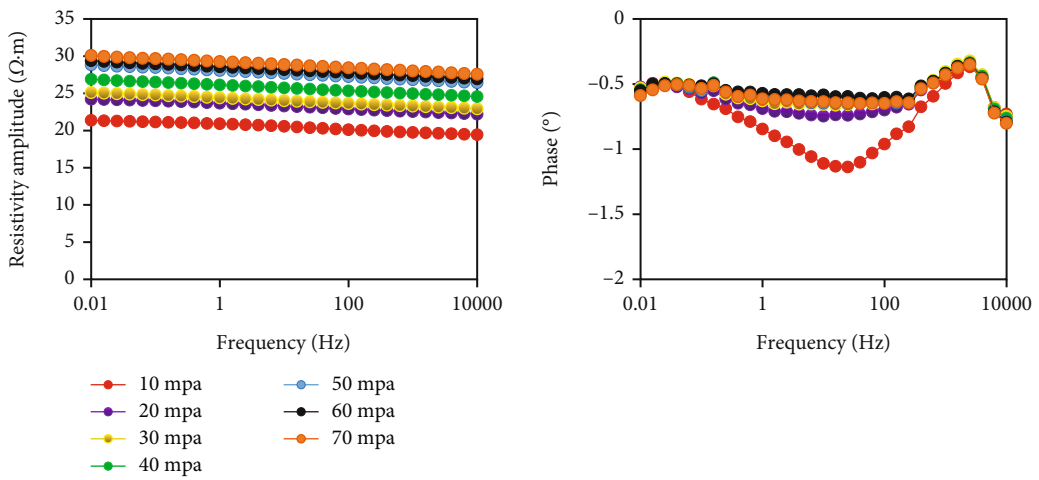

(c)

Figure 5: Continued.

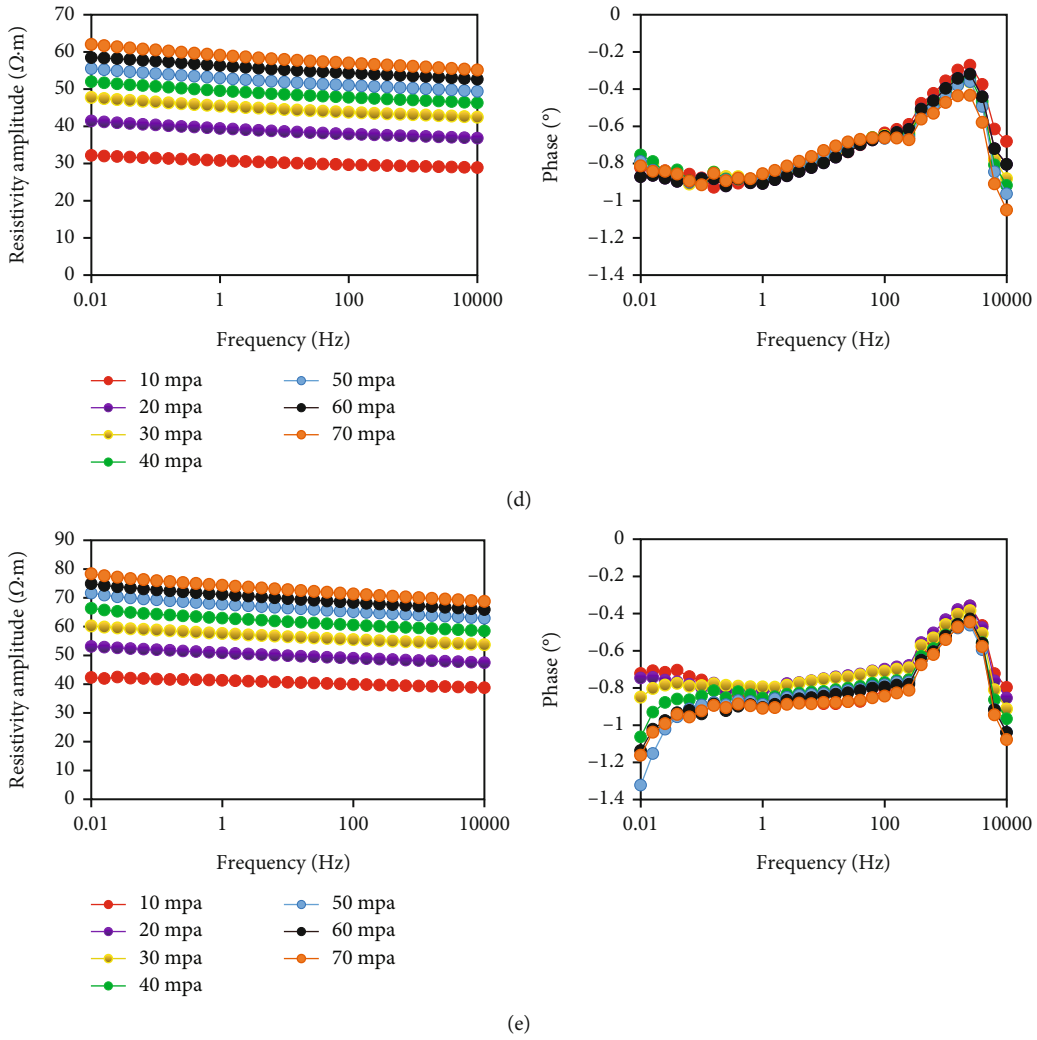

Figure 5: (a–e) The amplitude and phase curves of the complex resistivity of samples 1, 2, 3, 4, and 5 under variable pressures, respectively. The left column shows the complex resistivity amplitude curves, and the right column shows the complex resistivity phase curves.

simulate formation temperatures of up to 120°C and formation pressures of up to 70 MPa. It can accurately obtain the complex resistivity parameters of the core samples in the frequency range of 0.01 Hz to 1 MHz, and the low-frequency range of the complex resistivity is expanded by using the low-frequency characteristic of the 1260A impedance analyzer, which is more effective for the observation of the induced polarization [24]. The amplitude and phase of the complex resistivity, with frequencies of 0.01 Hz–10,000 Hz, of the five sandstone samples from the Huabei Oilfield were measured under normal temperature and pressure, variable temperature, variable pressure, and deepening conditions and also under different oil saturations. A schematic diagram of the equipment is shown in Figure 3.

2.3. Measurement Conditions and Complex Resistivity Model

2.3.1. Measuring Conditions

(1) Variable Pressure. The sample was saturated with 1% NaCl (10,000 ppm) solution and tested at 35°C under different pressure conditions. Due to the low pore pressure of 5 MPa, the formation pressure difference was simulated by changing the confining pressure. The experimental confining pressure ranged from 10 MPa to 70 MPa, and the test interval was 10 MPa. After the pressure was increased, the measurements were conducted after the sample became stable.

(2) Variable Temperature. The samples were saturated with 1% NaCl (10,000 ppm) solution and tested at different temperatures, a rock confining pressure of 60 MPa, and pore pressure of 5 MPa. The temperature ranged from 40°C to 100°C, and the test interval was 10°C. After the temperature was increased, the measurements were conducted after the sample became stable.

(3) Stratigraphic Conditions. The samples were saturated with 1% NaCl (10,000 ppm) solution, and the tests were conducted under simulated formation conditions. The simulated burial depths were 1000 m, 1500 m, 2000 m, 2500 m, and 3000 m. Based on the relationships between depth and temperature and pressure under formation conditions, the

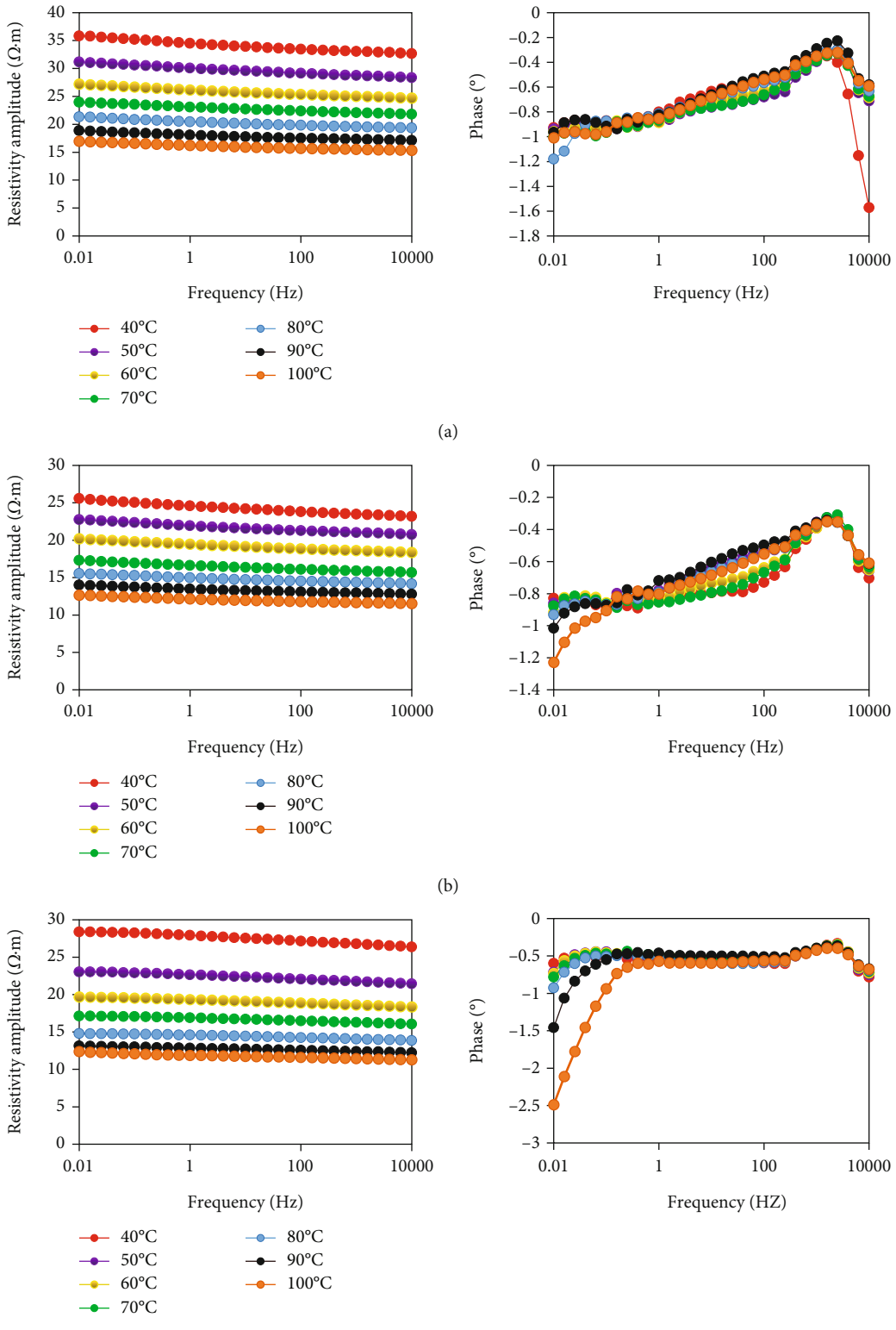

Figure 6: Continued.

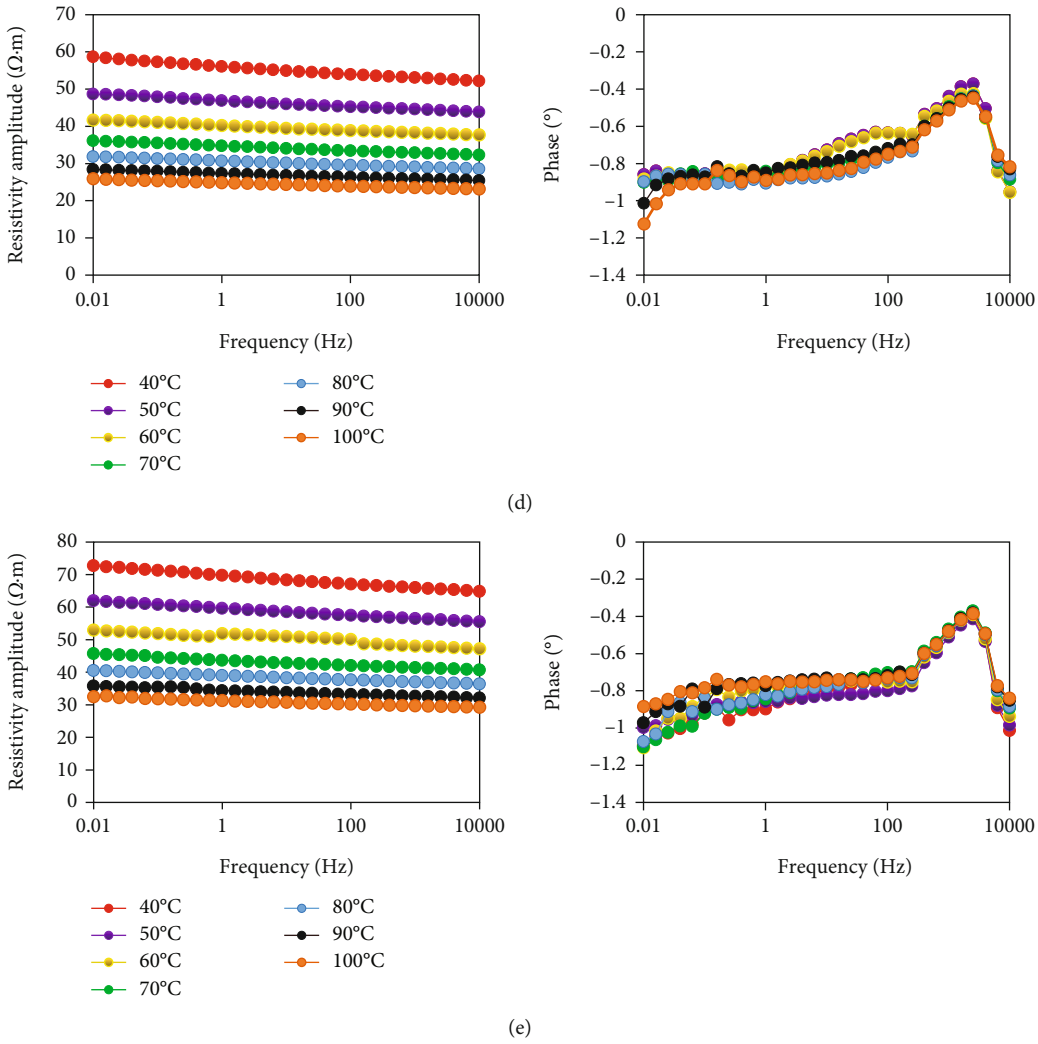

FIGURE 6: (a–e) The amplitude and phase curves of the complex resistivities of samples 1, 2, 3, 4, and 5 under variable temperature conditions, respectively. The left column shows the complex resistivity amplitude curves, and the right column shows the complex resistivity phase curves.

experimental conditions for simulating the corresponding formation depth were achieved by changing the temperature and pressure simultaneously. The relationships between depth and temperature and pressure under formation conditions are as follows:

$$T = 14 + 0.03(H - 20), \tag{1}$$

$$P_c = \rho g H = 10^{-3} \times 2.6 \times 9.8 \times H = 0.02548H, \tag{2}$$

where T is the temperature (°C), H is the formation depth (m), P_c is the confining pressure (MPa), ρ is density (g/cm^3), and g is the acceleration due to gravity (m/s^2).

(4) Variable Oil Saturation. The rock samples were displaced by oil under the condition of saltwater saturation, and the complex resistivities of the rock samples were measured under different oil (or water) saturation conditions.

2.3.2. Complex Resistivity Model. The Cole–Cole model describes the change in a rock's resistivity with frequency. Pelton [25] confirmed that the Cole–Cole model can be used to describe the change in a rock's resistivity with frequency, which laid a foundation for studying the IP effect. The expression is as follows:

$$\rho(\omega) = \rho_0 \left[1 - m\left(1 - \frac{1}{1 + (i\omega\tau)^c}\right)\right], \tag{3}$$

where $\rho(\omega)$ is the complex resistivity (Ω·m); ρ_0 is the direct current (DC) resistivity (Ω·m), m is the polarizability, τ is the time constant (s), and c is the frequency correlation coefficient. Based on the single Cole–Cole model, scholars have proposed other models through continuous improvement and development, such as the Dias model, the Debye model, and the multiple and compound Cole–

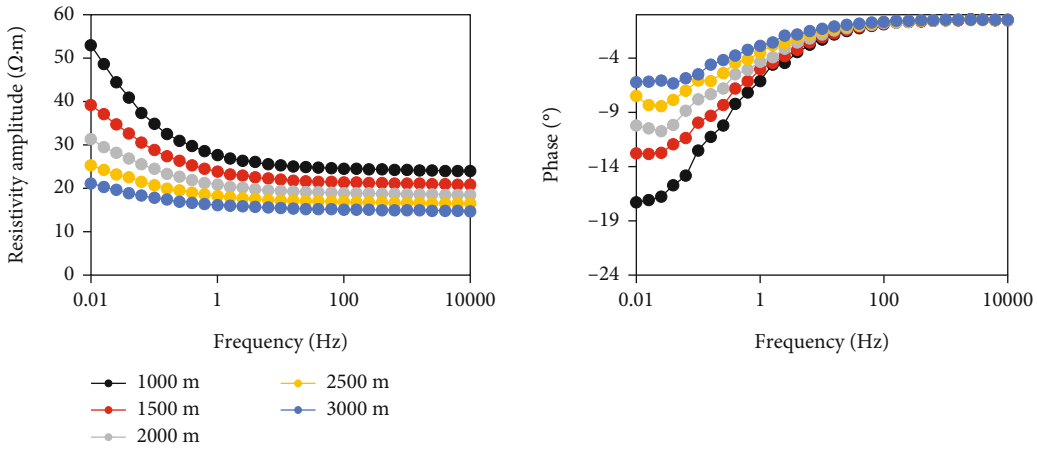

(a)

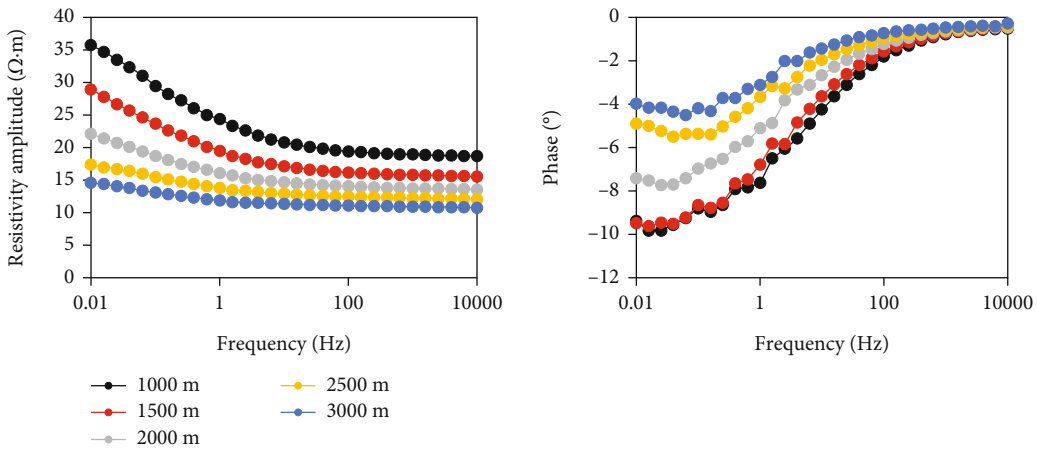

(b)

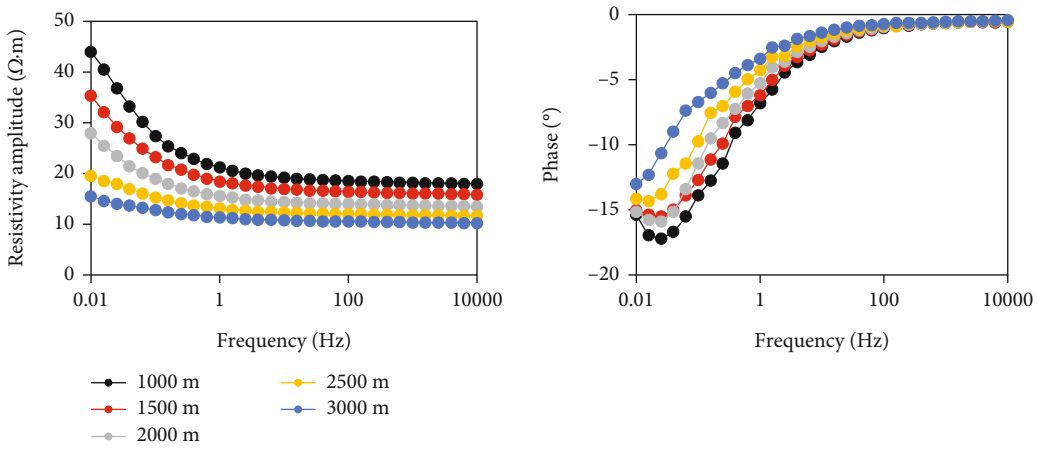

(c)

Figure 7: Continued.

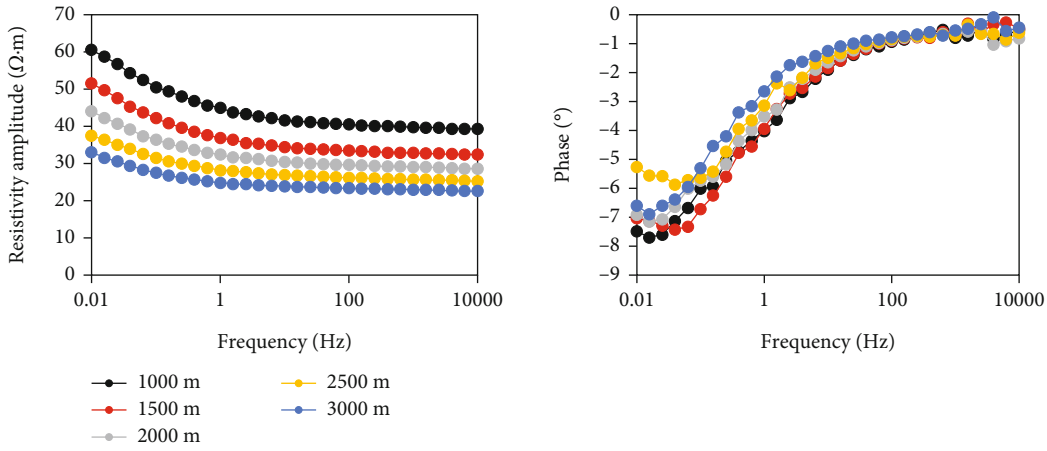

(d)

Figure 7: (a–d) The amplitude and phase curves of the complex resistivities of samples 1, 2, 3, and 5 under different simulated formation depths, respectively. The left column shows the complex resistivity amplitude curves, and the right column shows the complex resistivity phase curves.

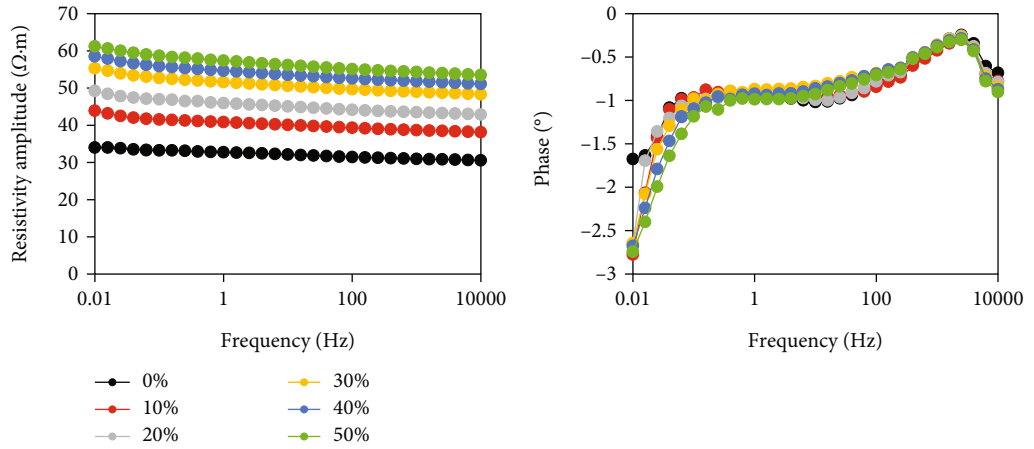

(a)

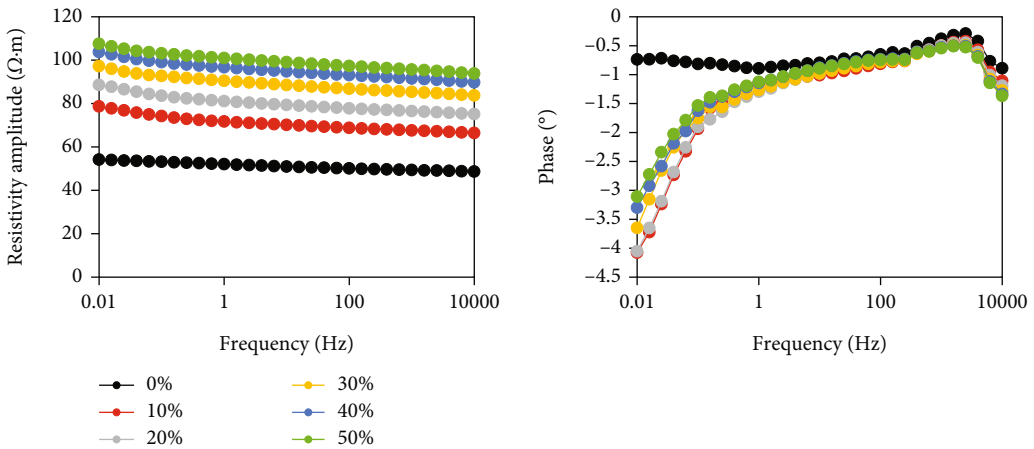

(b)

Figure 8: (a, b) The amplitude and phase curves of the complex resistivities of samples 1 and 5 under different oil saturation conditions, respectively. The left column shows the complex resistivity amplitude curves, and the right column shows the complex resistivity phase curves.

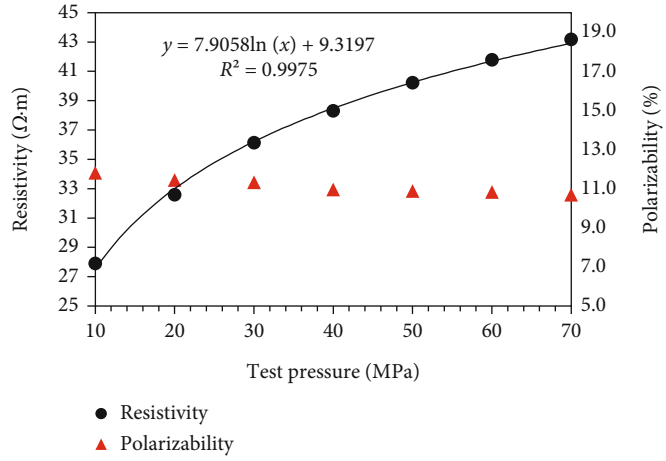

(a)

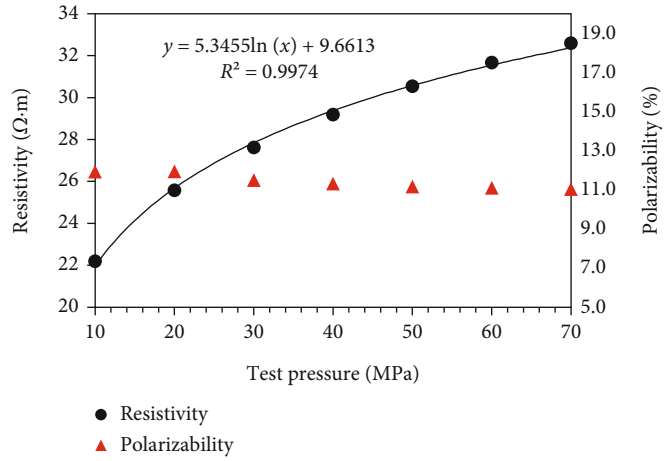

(b)

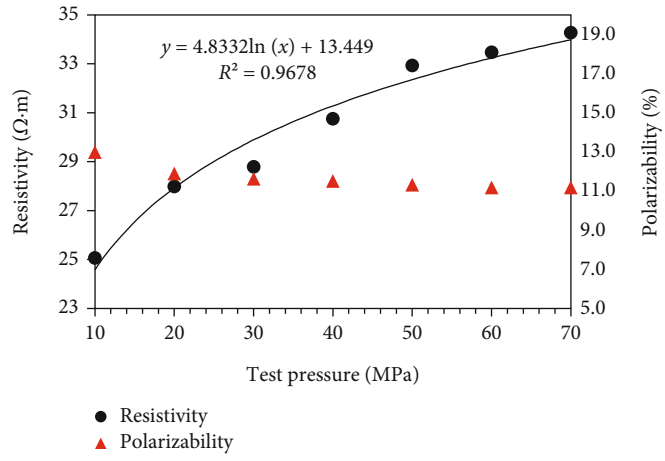

(c)

Figure 9: Continued.

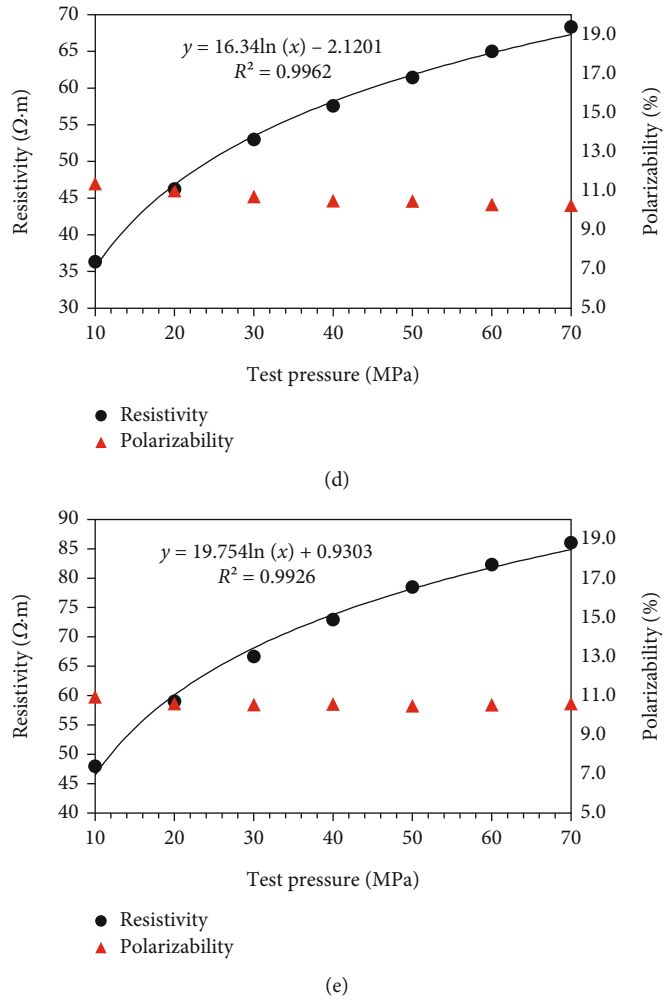

Figure 9: (a–e) The complex resistivity inversion results for samples 1, 2, 3, 4, and 5 under different pressure conditions, respectively.

Cole models. In this paper, the double Cole–Cole model is adopted:

$$\rho(\omega) = \rho_0\left\{1 - m_1\left[1 - \frac{1}{1 + (i\omega\tau_1)^{c_1}}\right] - m_2\left[1 - \frac{1}{1 + (i\omega\tau_2)^{c_2}}\right]\right\}, \tag{4}$$

where m_1, τ_1, and c_1 and m_2, τ_2, and c_2 are the spectrum parameters of the IP effect and electromagnetic effect, respectively. In this paper, the spectrum parameters (ρ_0, m_1, τ_1, and c_1), which reflect the characteristics of rock's induced polarization, are mainly studied [26].

3. Complex Resistivity Data under Different Measurement Conditions

3.1. Normal Temperature and Pressure Condition. The amplitude of the complex resistivities of the five sandstone samples measured under normal temperature and pressure conditions was 17 Ω·m to 43 Ω·m (Figure 4). The amplitude of the complex resistivity gradually increased with decreasing frequency, which is consistent with the real resistivity data. The curve changes greatly in the high-frequency and low-frequency regions. That is the absolute value of the phase suddenly increases with increasing frequency in the high-frequency region, while the absolute value of the phase initially decreases and then increases with decreasing frequency in the low-frequency region. Based on the mineral composition and physical property information for the rock samples, it was found that the resistivity amplitudes of the rock samples with smaller porosities and permeabilities were larger. Among the mineral components, the clay minerals had a large influence on the resistivities of the rock samples. Sample 5 had the lowest clay content, a weak formation water adsorption capacity, and a small porosity and permeability, and thus, it had the largest resistivity amplitude of all of the rock samples. In the phase spectrum curve of the complex resistivity, there is a peak in the low-frequency region and a peak in the high-frequency region, and the peak in the high-frequency region is mainly a manifestation of the Maxwell–Wagner interface polarization. This study investigated the characteristics of low-frequency electric polarization, which are closely related to the double electric layer between the rock particles and pore fluid.

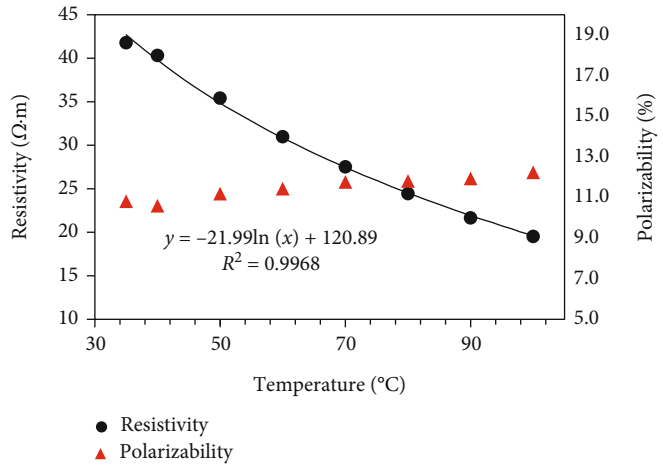

(a)

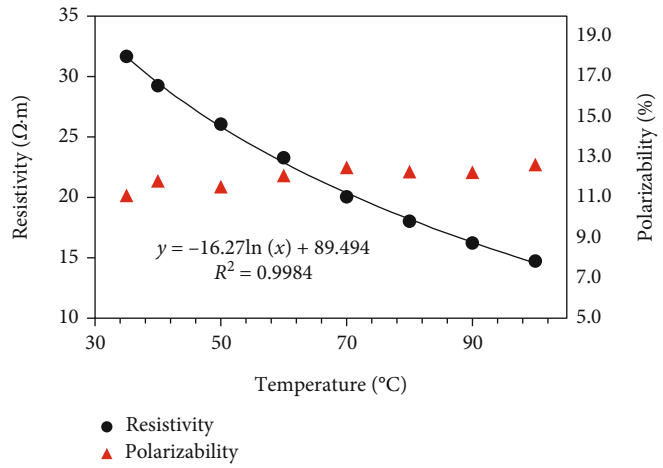

(b)

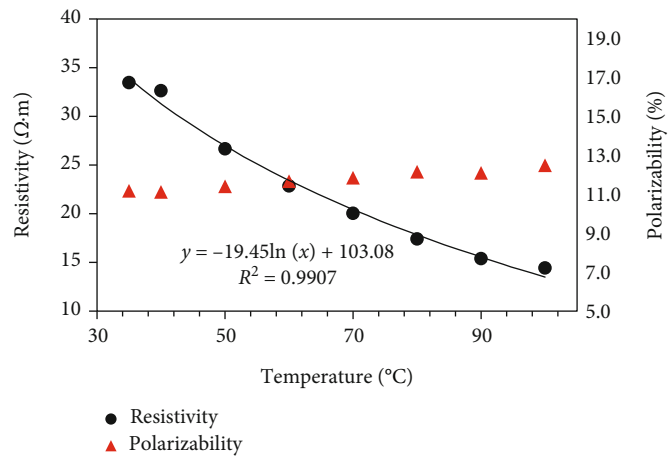

(c)

Figure 10: Continued.

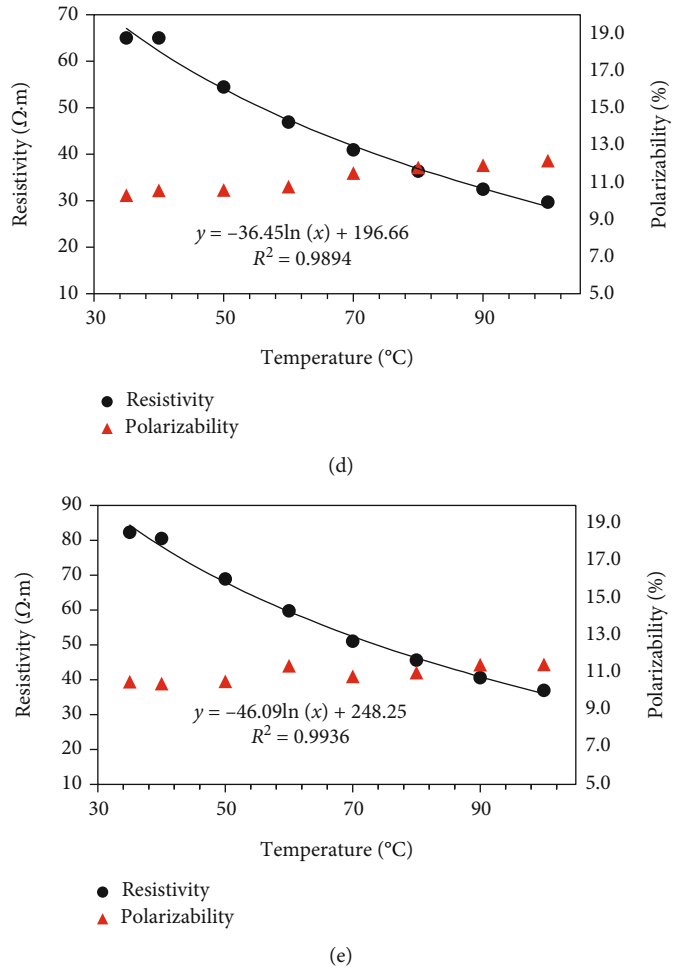

Figure 10: (a–e) The inversion results of the complex resistivity for samples 1, 2, 3, 4, and 5 under different temperature conditions, respectively.

3.2. Variable Pressure Conditions. According to the data for the five sandstone samples measured under different pressures, the amplitude of the complex resistivities of the tested samples increases with increasing pressure, but the shape of the frequency spectrum curve does not change significantly (Figure 5). This is consistent with the fact that the complex resistivity increases with decreasing frequency under normal temperature and pressure conditions. The phase curves also exhibit large changes in the low-frequency band and the high-frequency band, and the amplitude of the absolute value of the phase appears in the low-frequency band.

The variation characteristics of the complex resistivity amplitude with pressure are closely related to the pore structure of the rock, and the temperature remains unchanged. With increasing pressure, the contact between the particles in the rock becomes closer and closer, and the pore structure changes (i.e., the pores become smaller), which even leads to the closure of some of the pores, and the communication between pores is blocked, thus affecting the migration of the conductive particles in the pore fluid and resulting in a decrease in the conductivity of the rock and an increase in the resistivity.

3.3. Variable Temperature Conditions. Based on the measurements collected at different temperatures, the amplitude of the complex resistivity decreases with increasing temperature, and the amplitude of the complex resistivity decreases more with increasing temperature in the lower-temperature range than in the high-temperature range (Figure 6). The phase curve shows that the absolute value of the phase increases with decreasing frequency in the low-frequency band, and there is a strong change in the high-temperature band.

The temperature mainly affects the complex resistivities of the rock samples by affecting the velocity of the conductive particles in the pore fluid. With increasing temperature, the conductive particles in the fluid (i.e., ions, electrons, and other conductive media) in the rock pores move faster, which leads to an increase in the conductivity and a decrease in the resistivity of the rock sample.

3.4. Different Simulated Depth Conditions. The complex resistivity data for the sandstone measured under different simulated depths show that the amplitude of the complex resistivity decreases gradually with increasing depth (Figure 7). Under other measurement conditions, the amplitude of the

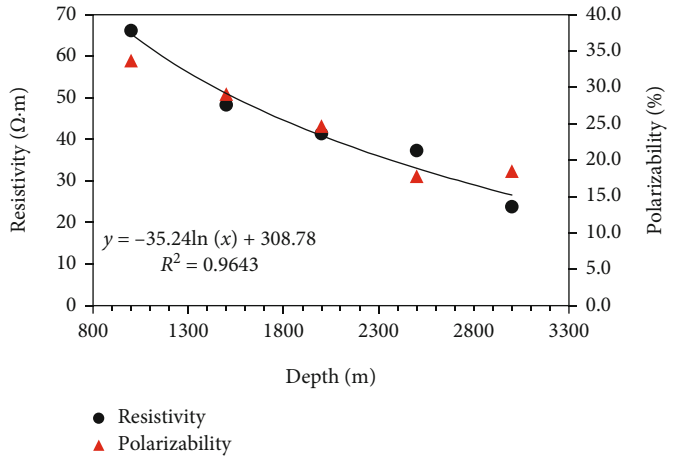

(a)

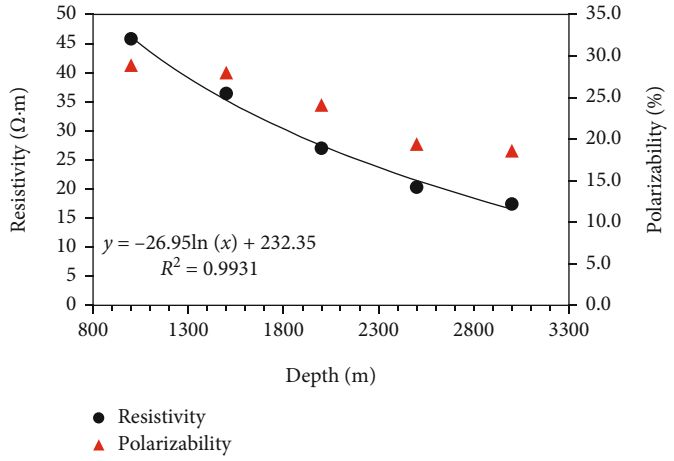

(b)

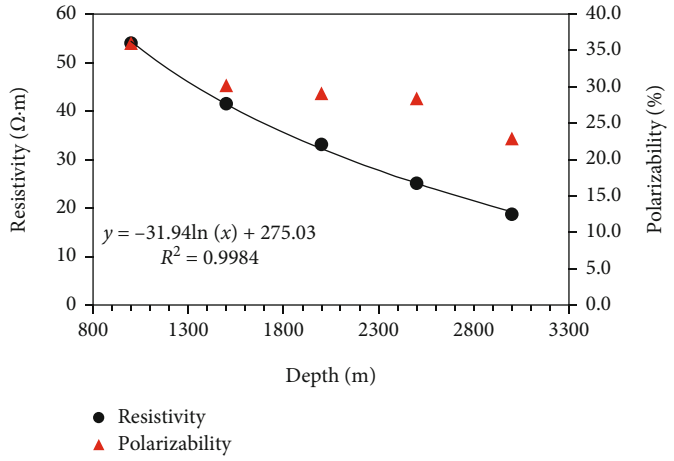

(c)

Figure 11: Continued.

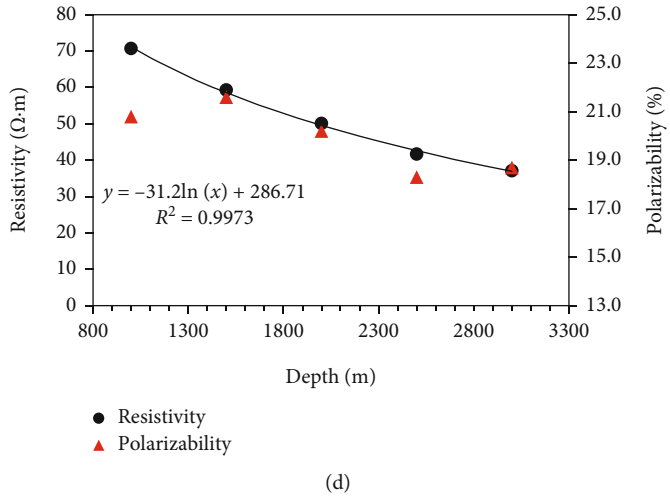

FIGURE 11: (a–d) The inversion results of the complex resistivity of samples 1, 2, 3, and 5 for different simulated depths, respectively.

complex resistivity changes gently with the frequency, while the spectrum curve of the complex resistivity amplitude at different depths exhibits a relatively large change in the low-frequency region, and the amplitude of the complex resistivity increases with decreasing frequency. With increasing simulation depth, the temperature and pressure both increase, while the resistivity amplitude decreases, which indicates that within the experimental conditions tested in this study, the effect of the temperature on enhancing the conductivity by increasing the velocity of the conductive particles is greater than that of the pressure on decreasing the conductivity by compressing the pores. The phase value initially decreases and then increases gradually with increasing frequency.

3.5. Different Saturation Conditions. According to the measured data, under different oil saturation conditions, the amplitude of complex resistivity gradually increases with the increase of oil saturation (Figure 8). On the other hand, the phase curve shows that the amplitude of the low-frequency band changes greatly, and the absolute value of the phase gradually increases with the decrease in frequency.

4. Results and Discussion

According to the complex resistivity data measured under various conditions, the low-frequency band (0.01 Hz–100 Hz) was used for the inversion. We extracted four IP parameters, namely, the DC resistivity (ρ_0), polarizability (m_1), time constant (τ_1), and frequency correlation coefficient (c_1) [27], and we vigorously analyzed the influences of the different conditions on the resistivity and polarizability of the sandstone.

4.1. Inversion Results under Different Pressure Conditions. According to the inversion results, under different pressure conditions, the resistivity of the five sandstone samples increases logarithmically with increasing pressure, while the polarizability decreases to some extent with increasing pressure (Figure 9). As the pressure increases, the rock particles become closer together, the pore structure changes, and the fluid in the pores is squeezed out, resulting in a reduction of the electric double layer on the surface of the rock particles and a reduction of the surface area where the IP effect can occur, and thus, the polarizability decreases to some extent.

4.2. Inversion Results under Different Temperature Conditions. According to the inversion results of the complex resistivity data for the five sandstone samples under different temperature conditions, the resistivity of the sandstone samples decreases logarithmically with increasing temperature, while the polarizability increases with increasing temperature (Figure 10).

As the test temperature increases, the movement speed of the conductive particles in the pore fluid of the rock increases, which increases the conductivity and decreases the resistivity. However, when the temperature increases to a certain level, the rock particles thermally expand, and the pore structure is affected, which reduces the variation trend of the resistivity curve.

4.3. Inversion Results at Different Depths. According to the inversion results, when the IP parameter information about the rock samples is extracted from under simulated stratum conditions, the resistivity of the rock samples decreases logarithmically with increasing depth, while the polarizability decreases to a great extent with increasing depth (Figure 11). Generally, with increasing formation depth, the temperature and pressure of the reservoir rock increase. The above experimental results show that the polarizability decreases with increasing pressure and increases with increasing temperature. However, when the depth increases, the polarizability decreases when the temperature and pressure increase simultaneously, indicating that the influence of the pressure on the polarizability is greater than that of the temperature. This is mainly reflected in the fact that the influences of the porosity and pore structure on the polarizability are greater than the influence of the temperature. Of

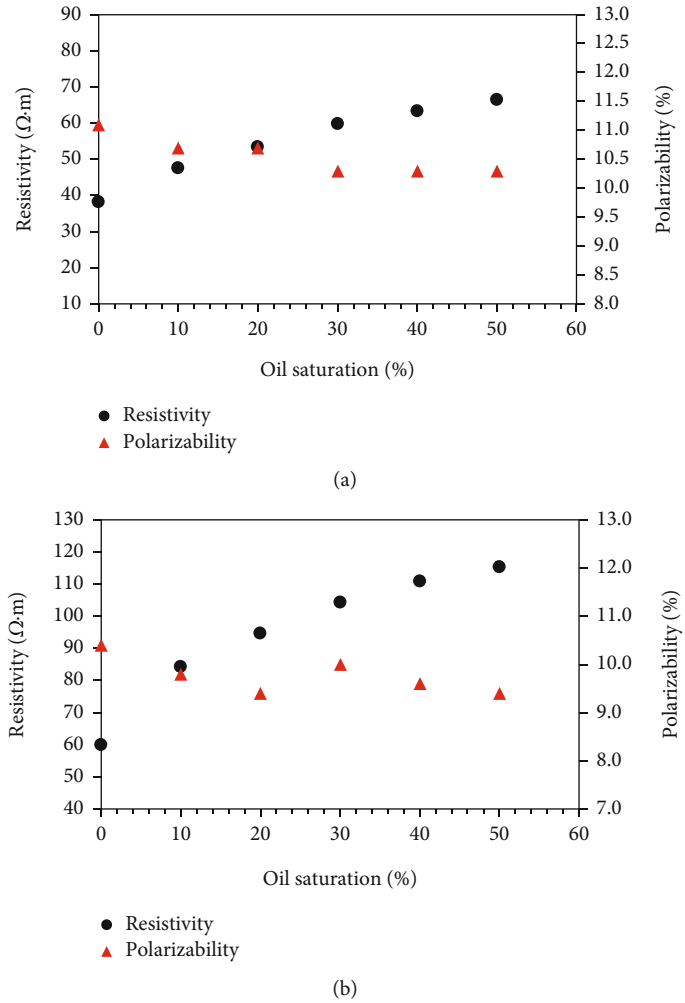

Figure 12: (a, b) The inversion results of the complex resistivity of samples 1 and 5 under different oil saturation conditions, respectively.

course, there are many factors affecting the polarizability, and only the temperature and pressure are considered here.

4.4. Inversion Results under Different Saturation Conditions. The inversion results for the rock samples under different oil saturation conditions show that with increasing oil saturation, the resistivity increases logarithmically, while the polarizability decreases overall (Figure 12). As the oil saturation increases, the pore fluid is gradually replaced by the displacement oil, resulting in a gradual increase in resistivity.

Through comparative analysis of the complex resistivity data under different measurement conditions, it was found that the complex resistivity value under each measurement condition increases or decreases logarithmically, that is,

$$y = a \ln x + b. \tag{5}$$

The absolute value of coefficient a reflects the speed of the logarithmic change; that is, the larger the absolute value of a is, the greater the influence of the measurement conditions on the resistivity is. Based on the above-described experimental data, it was found that the burial depth has the greatest influence on the resistivity, followed by temperature and finally pressure.

5. Conclusions

(1) Complex resistivity data for reservoir rocks were obtained by measuring the complex resistivity of sandstone samples under various conditions, such as normal temperature and pressure conditions, variable temperature conditions, different depths (simulated formation conditions), and different oil saturations; and the influences of the different measurement conditions on the induced polarization characteristics of the sandstone reservoir were determined

(2) Based on the inversion of a complex resistivity model, the IP parameters under different measurement conditions were extracted. Through analysis, it was found that the resistivity increases logarithmically with increasing pressure, decreases logarithmically with increasing temperature, decreases logarithmically with increasing depth, and increases logarithmically with increasing oil saturation. Depth has the greatest

influence on resistivity, followed by temperature and pressure. The polarizability decreases slightly with increasing pressure and increases slightly with increasing temperature, but the amplitude only changes slightly. In addition, the polarizability decreases obviously with increasing depth, and the overall polarizability decreases with increasing oil saturation

(3) The study of the complex resistivity characteristics of sandstone reservoirs under different measurement conditions is helpful for analyzing the electrical response characteristics of sandstone reservoirs from multiple angles and provides more comprehensive basic data for fluid identification and the evaluation of complex reservoirs. Currently, the lithology of the reservoir rocks tested is relatively simple. In future research, additional rock samples from different regions and with different lithologies will be tested to improve the research on the complex resistivity characteristics of the reservoir rocks

Data Availability

The data used to support the findings of this study are available from the corresponding author upon request.

Conflicts of Interest

The authors declare no conflict of interest.

Acknowledgments

The authors are grateful to the National Natural Science Foundation of China (No. 42174083, No. 42030805, and No. 42274087). We thank the department of geophysical and geochemical prospecting, BGP, CNPC, for supplying shale samples and data.

References

[1] D. J. Marshall and T. R. Madden, "Induced polarization, a study of its causes," *Geophysics*, vol. 24, no. 4, pp. 790–816, 1959.

[2] J. Gao, Q. Feng, and Y. Sun, "Electrode-type complex resistivity logging and its application," *Acta Petrolei Sinica*, vol. 24, no. 4, pp. 62–64, 2003.

[3] J. H. Norbisrath, R. J. Weger, and G. P. Eberli, "Complex resistivity spectra and pore geometry for predictions of reservoir properties in carbonate rocks," *Journal of Petroleum Science and Engineering*, vol. 151, pp. 455–467, 2017.

[4] M. A. Khalil, "Real surface conductivity component as indicator for the hydraulic conductivity," *Arabian Journal of Geosciences*, vol. 4, no. 1-2, pp. 269–281, 2011.

[5] K. Xiang, L. J. Yan, and H. Hu, "Relationship analysis between brittle index and electrical properties of marine shale in South China," *Geophysical Prospecting for Petroleum*, vol. 55, no. 6, pp. 894–903, 2016.

[6] S. Zargari, K. L. Canter, and M. Prasad, "Porosity evolution in oil-prone source rocks," *Fuel*, vol. 153, pp. 110–117, 2015.

[7] M. Zhdanov, "Generalized effective-medium theory of induced polarization," *Geophysics*, vol. 73, no. 5, pp. F197–F211, 2008.

[8] J. J. Li, S. G. Deng, Y. R. Fan, and D. Sun, "Study on influential factors on core's complex resistivity," *Well Logging Technology*, vol. 13, no. 3, pp. 11–15, 2005.

[9] K. F. Shi, L. P. Wu, and S. H. Li, "Determine and regularity of reservoir rock sample electricity parameter," *Acta Geophysica Sinica*, vol. 38, no. S1, pp. 295–302, 1995.

[10] M. Schmutz, A. Revil, P. Vaudelet, M. Batzle, P. F. Viñao, and D. D. Werkema, "Influence of oil saturation upon spectral induced polarization of oil-bearing sands," *Geophysical Journal International*, vol. 183, no. 1, pp. 211–224, 2010.

[11] A. Revil, M. Schmutz, and M. L. Batzle, "Influence of oil wettability upon spectral induced polarization of oil-bearing sands," *Geophysics*, vol. 76, no. 5, pp. A31–A36, 2011.

[12] V. Burtman and M. S. Zhdanov, "Induced polarization effect in reservoir rocks and its modeling based on generalized effective-medium theory," *Resource-efficient Technologies*, vol. 1, no. 1, pp. 34–48, 2015.

[13] J. Jiang, S. Z. Ke, R. Rezaee, J. J. Li, and F. Wu, "The frequency exponent of artificial sandstone's complex resistivity spectrum," *Geophysical Prospecting*, vol. 69, no. 4, pp. 856–871, 2021.

[14] W. F. Brace and A. S. Orange, "Further studies of the effects of pressure on electrical resistivity of rocks," *Journal of Geophysical Research*, vol. 73, no. 16, pp. 5407–5420, 1968.

[15] Y. Liu, Q. Sun, J. J. Hu, and C. B. Li, "Effects of temperature and pressure on electrical conductivity and wave velocity of basalt: a review," *Acta Geodaetica et Geophysica*, vol. 56, no. 1, pp. 177–191, 2021.

[16] B. Li, T. C. Han, L. Y. Fu, and Y. Han, "Pressure effects on the anisotropic electrical conductivity of artificial porous rocks with aligned fractures," *Geophysical Prospecting*, vol. 70, no. 4, pp. 790–800, 2022.

[17] B. Sun, X. G. Tang, K. Xiang, and C. X. Dou, "The analysis and measure on complex resistivity parameters of shaly sands in high temperature and high pressure," *Chinese Journal of Engineering Geophysics*, vol. 13, no. 3, pp. 277–284, 2016.

[18] L. Z. Cheng, Y. Wang, and C. Zhang, "Anisotropy of complex resistivity of the shale in eastern Guizhou province and its correlations to reservoir parameters of shale gas," *Chinese Journal of Geophysics*, vol. 64, no. 9, pp. 3344–3357, 2021.

[19] J. Wang, C. Y. Lu, Y. H. Hu, and Z. G. Sun, "Experiment of rock resistivity under formation conditions," *Petroleum Exploration and Development*, vol. 31, no. 1, pp. 113–115, 2004.

[20] K. Amalokwu and I. H. Falcon-Suarez, "Effective medium modeling of pressure effects on the joint elastic and electrical properties of sandstones," *Journal of Petroleum Science and Engineering*, vol. 202, p. 108540, 2021.

[21] W. D. Qian, T. J. Yin, and G. W. Hou, "A new method for clastic reservoir prediction based on numerical simulation of diagenesis: a case study of Ed1 sandstones in Bozhong depression, Bohai Bay basin, China," *Advances in Geo-Energy Research*, vol. 3, no. 1, pp. 82–93, 2019.

[22] Y. Luo, K. Xiang, L. Yan et al., "Influence of wettability upon IP characteristics of rocks in low porosity and low permeability reservoirs," *Journal of Petroleum Science and Engineering*, vol. 216, p. 110752, 2022.

[23] J. C. Cai, L. X. Zhao, F. Zhang, and W. Wei, "Advances in multiscale rock physics for unconventional reservoirs," *Advances in Geo-Energy Research*, vol. 6, no. 4, pp. 271–275, 2022.

[24] K. Xiang, W. B. Hu, L. J. Yan, X. G. Tang, and G. Yu, "Study on measurement technology and calibration method of rock complex resistivity," *Science Technology and Engineering*, vol. 16, no. 5, pp. 138–141, 2016.

[25] W. H. Pelton, *Interpretation of Induced Polarization and Resistivity Data*, University Utah, Utah, 1977.

[26] K. Xiang, L. J. Yan, Z. G. Wang, and Y. Lu, "Comprehensive physical properties and exploration potential of the Permian igneous rocks in the southwestern Sichuan Basin," *Minerals*, vol. 12, no. 7, p. 789, 2022.

[27] K. Xiang, W. B. Hu, L. J. Yan et al., "Complex resistivity dispersion characteristics of shale samples in Sichuan and Guizhou area," *Oil Geophysical Prospecting*, vol. 49, no. 5, pp. 1013–1019, 2014.